PNAS
www.pnas.org

Supplementary Information for

The *Drosophila* chemokine-like Orion bridges phosphatidylserine and Draper in phagocytosis of neurons

Hui Ji[1], Bei Wang[1], Yifan Shen[1], David Labib[1,3], Joyce Lei[1,4], Xinchen Chen[1], Maria Sapar[1,3], Ana Boulanger[2], Jean-Maurice Dura[2] and Chun Han[1,*]

[1]Weill Institute for Cell and Molecular Biology and Department of Molecular Biology and Genetics, Cornell University, Ithaca, NY 14853, USA
[2] IGH, Univ Montpellier, CNRS, Montpellier, France
[3]Current address: The New York Stem Cell Foundation Research Institute, New York, NY 10019, USA
[4]Current address: Tisch MS Research Center of New York, New York, NY 10019, USA
[*]Correspondence: chun.han@cornell.edu

This PDF file includes:

Other supplementary materials for this manuscript include the following:

SI Methods

Molecular cloning and transgenic flies

orion-mNG2$_{11x4}$-V5-T2A-LexA: Two copies of a gRNA spacer sequence targeting *orion* C-terminus and 3'UTR (Table S2) were cloned into pAC-CR7T-gRNA2.1-nlsBFP (Addgene 170515) according to published protocols (1). The resulting plasmid was digested by PstI and NheI and assembled with four DNA fragments (through NEBuilder HiFi DNA assembly, New England Biolabs, Inc) to make an *orion* gRNA-donor vector. The four DNA fragments include a T2A-LexA-VP16 fragment that was PCR-amplified from pUC57-50-GS-FRTGFP2ALexAVP16-50 (2) (a gift from Larry Zipursky), an mNG2$_{11x4}$-V5 DNA fragment (synthesized by Integrated DNA Technologies, Inc.), and 5' and 3' homology arms (surrounding the stop codon of *orion*, ~1 kb each) that were PCR-amplified from the genomic DNA of *w^{1118}*.

UAS-orionA-GFP: OrionA coding sequence (CDS) was PCR-amplified from cDNA clone LD24308 (*Drosophila* Genomics Resource Center) and assembled with a superfolder GFP (sfGFP) fragment into pIHEU-MCS (Addgene 58375) (3), resulting in pIHEU-orionA-GFP.

UAS-orionB-GFP: The first two exons of *orionB*, together with the first intron, was PCR-amplified from *w^{1118}* genomic DNA. The common CDS of OrionA and OrionB was PCR-amplified from LD24308. Both fragments were assembled into pIHEU-orionA-GFP to replace the orionA CDS, resulting in pIHEU-orionB-GFP.

UAS-orionB-CD2-mIFP: A pACU-CD2-mIFP plasmid was first constructed in pACU (Addgene 58373) (4). The CDS of CD2-mIFP contains, from the N-terminus to the C-terminus, the rat CD2 CDS (AA24 to AA344), mIFP CDS (5), and Kir2.1 ER exit signal (4). The OrionB CDS was then inserted before CD2 to make pACU-orionB-CD2-mIFP.

UAS-orionB^{AX3C}-GFP: An OrionB^{AX3C} coding fragment was amplified from pENTR-orionB-AX$_3$C (6) and used to replace OrionB in pIHEU-orionB-GFP, resulting in pIHEU-orionB-AX$_3$C-GFP.

UAS-orionB^{AAY}-GFP: The RRY motif in OrionB coding sequence was changed into AAY by mutagenesis PCR. The mutated OrionB fragment was used to replace OrionB in pIHEU-orionB-GFP, resulting in pIHEU-orionB-AAY-GFP.

UAS-orionB^{1}-GFP: A G611D mutation was introduced into OrionB sequence by overlap-extension PCR. The mutated OrionB fragment was used to replace OrionB in pIHEU-orionB-GFP, resulting in pIHEU-orionB-G611D-GFP.

LexAop-orionB-GFP: The OrionB-sfGFP CDS was inserted into KpnI/XbaI sites of pAPLO vector (7).

UAS-Drpr$^{\Delta Cyto}$: The extracellular domain and transmembrane domain of Drpr (AA1 to AA827) was PCR-amplified from *UAS-drpr-I* (8) genomic DNA. An smFP-HA (non-fluorescent) fragment was PCR-amplified from pCAG-smFP-HA (9) (a gift from Loren Looger). The two fragments were cloned into pACU through restriction cloning, resulting in pACU-DrprTM_smGFP(dark).

UAS-smNG2$_{1-10}$: An mNG2$_{1-10}$ fragment was synthesized (Integrated DNA Technologies, Inc.) and cloned into NheI/XbaI-digested pIHEU-sfGFPLactC1C2 (3), resulting in pIHEU-smNG2(1-10).

UAS-CDC50-T2A-ATP8A(E): The CDS of ATP8A isoform E (ATP8A(E)) was PCR-amplified from cDNA clone GH28327 (*Drosophila* Genomics Resource Center) and cloned into EcoRI/XbaI sites of pACU. The ATP8A(E) sequence is preceded by PacI and NheI sites and followed by a FLAG tag and a Kir2.1 ER exit signal (3). In parallel, the CDC50 CDS was PCR-amplified from NB40 cDNA library

(10) (a gift from Xinhua Lin) and cloned into EcoRI/XbaI sites of pACU. The CDC50 sequence is preceded by a PacI site and followed by BglII and NheI sites. A T2A fragment generated by annealed oligos was then inserted into the BglII/NheI sites. The CDC50-T2A (PacI/NheI) fragment was then released and cloned into PacI/NheI sites before ATP8A(E), resulting in pACU-CDC50-T2A-ATP8A(E).

drpr-GFP: The sfGFP CDS was inserted seamlessly before the stop codon of Drpr-PE in BAC clone CH321-16B09 according to published protocols of recombineering (11). Briefly, the *galK* CDS was first inserted before the stop codon of Drpr-PE in CH321-16B09 in bacterial strain SW102 through *galK*-mediated positive selection. The sfGFP CDS was then used to replace *galK* CDS in SW102 through *galK*-mediated negative selection. The resulting construct was transferred to bacterial strain EPI300 for propagation.

drpr-mNG: A *drpr-mNG* KI donor vector was constructed by assembling a pBluescript backbone and four DNA fragments. The four DNA fragments include the mNG CDS (12), a 3xP3-GFP selection marker modified from pHD-DsRed (Addgene #51434), and 5' and 3' homology arms (surrounding the stop codon of Drpr-PE, ~1 kb each) that were PCR-amplified from CH321-16B09. A dual gRNA expression vector was constructed in pCFD4-U6.1_U6.3 (13) to target the C-terminus and 3' UTR of *drpr* (Table S2).

gRNA-orion and *gRNA-orion-drpr*: A dual gRNA vector targeting *orion* and a quadruple gRNA vector targeting both *orion* and *drpr* were constructed in pAC-U63-QtgRNA2.1-BR (Addgene 170513) according to published protocols (1).

Transgenic constructs were injected by Rainbow Transgenic Flies to transform flies through φC31 integrase-mediated integration into attP docker sites.

Generation of KI flies

To generate *drpr-mNG*, *drpr* KI donor vector and gRNA-expression vector were co-injected in *Act-Cas9* embryos. Adult flies from injected embryos were crossed to *w1118; TM3/TM6B*. The progeny was screened for green fluorescence in the adult eye. GFP-positive candidates were crossed to $y^1\ w^{67c23}\ Cre(y+)^{1b};\ D/TM3,\ Sb^1$ (BDSC, #851) to remove 3xP3-GFP. GFP-negative candidates were made isogenic and the mNG insertion was confirmed by genomic PCR and sequencing.

To generate *orion-mNG2*$_{11x4}$*-V5-T2A-LexA*, the *orion* gRNA-donor vector was injected into y^1 *nos-Cas9*$^{ZH\text{-}2A}$ w^* (BDSC, #54591) embryos. Adult flies from injected embryos were crossed to $y^1\ w^*;$ *13XLexAop2-6XGFP*^{attP2}*/TM6B* (BDSC, #52266). GFP-positive female candidates from the progeny were collected to cross with $y^1\ w^*;$ *TM3/TM6B*. The adult progeny was then screened for GFP-positive males that were white-eyed and RFP-negative (i.e. having no *nos-Cas9*$^{ZH\text{-}2A}$). The males were then crossed to FM6 to remove *13XLexAop2-6XGFP*^{attP2} and to establish isogenic stocks. The -mNG211x4-V5-T2A-LexA insertion is verified by genomic PCR and sequencing.

CRISPR-TRiM

The efficiency of transgenic gRNA lines was validated by the Cas9-LEThAL assay (14). Homozygous males of each gRNA line were crossed to *Act-Cas9 w lig4* (BDSC, #58492) homozygous females. *gRNA-orion* crosses yielded viable female progeny and male lethality between 3rd instar larvae to prepupae; *gRNA-drpr* crosses resulted in lethality in late pupae; *gRNA-orion-drpr* crosses yielded viable female progeny and male lethality before wandering 3rd instar larvae. These results suggest that all gRNAs are efficient.

C4da-specific gene knockout was carried out using *ppk-Cas9* (14). Tissue-specific knockout in da neuron precursor cells was carried out with *SOP-Cas9* (14). Tissue-specific knockout in pan-epidermal cells was carried out using *shot-Cas9 (15)*. Tissue-specific knockout in epidermal cells in the posterior half of each segment was carried out using *hh-Cas9* (14). Whole-animal knockout was carried out using *Act-Cas9* (13).

Live imaging

Animals were reared at 25°C in density-controlled vials (60-100 embryos/vial) on standard yeast-glucose medium (doi:10.1101/pdb.rec10907). Larvae at 96 hours AEL (3rd instar larval stage) or stages specified were mounted in 100% glycerol under coverslips with vacuum grease spacers and imaged using a Leica SP8 microscope equipped with a 40X NA1.30 oil objective. Larvae were lightly anesthetized with isoflurane before mounting. For consistency, we imaged dorsal ddaC neurons from A1-A3 segments (2-3 neurons per animal) on one side of the larvae. Unless stated otherwise, confocal images shown in all figures are maximum intensity projections of z stacks encompassing the epidermal layer and the sensory neurons beneath, which are typically 8–10 μm for 3rd instar larvae.

Injury assay

Injury assay at the larval stage was done as described previously (3). Briefly, larvae at 84 hrs AEL were lightly anesthetized with isoflurane, mounted in a small amount of halocarbon oil under coverslips with grease spacers. The laser ablation was performed on a Zeiss LSM880 Confocal/Multiphoton Upright Microscope, using a 790 nm two-photon laser at primary dendrites of ddaC neurons in A1 and A3 segments. Animals were recovered on grape juice agar plates following lesion for appropriate times before imaging.

Long-term time-lapse imaging

Long-term time-lapse imaging at the larval stage was done as described previously (3, 15). Briefly, a layer of double-sided tape was placed on the coverslip to define the position of PDMS blocks. A small amount of UV glue was added to the groove of PDMS and to the coverslip. Anesthetized larvae were placed on top of the UV glue on the coverslip and then covered by PDMS blocks with the groove side contacting the larva. Glue was then cured by 365nm UV light. The coverslip with attached PDMS and larvae was mounted on an aluminum slide chamber that contained a piece of moistened Kimwipes (Kimtech Science) paper. Time-lapse imaging was performed on a Leica SP8 confocal equipped with a 40x NA1.3 oil objective and a resonant scanner at digital zoom 0.75 and a 3-min interval. For imaging after ablation, larvae were pre-mounted in the imaging chamber and subjected to laser injury. The larvae were then imaged 1-2 hours after ablation.

Pinching assay

Larvae at 96 hrs AEL were lightly anesthetized with isoflurane. Gentle pinching was performed at A2 or A3 segment and near the dorsal midline of larvae using a pair of forceps (DUMONT # 3, Fisher Scientifics) without cracking the cuticle. The pinched larvae were imaged after a 2-hr recovery.

Immunohistochemistry

Immunostaining of *Drosophila* larvae was performed as previously described (7). Briefly, 3rd instar larvae were dissected in cold PBS, fixed in 4% formaldehyde/PBS for 20 min at room temperature (RT), and stained with the proper primary antibodies (Table S1) for 2 hrs at RT and subsequent secondary antibodies (Table S1) for 2 hrs at RT.

Protein purification

All the steps were carried out either on ice or at 4°C. 2 mL Ni-NTA Resin (ThermoFisher) was washed with lysis buffer (50 mM Tris-HCl (pH 7.5), 150 mM NaCl, 10% glycerol, 10 mM imidazole) three times for 5 min at 800x g. 125µL Ni-NTA Resin was washed with 1 mL PBS for three times at 800x g for 5 min. Purified 6xHis nanobody was thawed on ice and incubated with Ni-NTA Resin on a rotor for 1 hr. 50 *Drosophila* larvae (*Dcg-Gal4>UAS-OrionB-GFP*) were frozen at –80°C and thawed on ice. 300 µL of lysis buffer and 200 µL of 10 x protease inhibitor cocktail (Promega), 10 µL AEBSF (200x) (ThermoFisher) and 5 ceramic beads (Omni International) were added to the tube and homogenized using a beater (Omni International) for 3 times (30s beating, 30s on ice) at level 4. Another 500µL lysis buffer, 10 µL 10% TritonX-100 and 10 µL AEBSF (200x) (ThermoFisher) was added to the tube and centrifuged at 10,000x g for 10 min. 700 µL supernatant was added to 2 mL Ni-NTA Resin and incubated for 1 hr. The mixture was centrifuged at 800x g for 5 min. The flowthrough was then incubated in Ni-NTA-6xHis-nanbody for another hour and centrifuged at 800x g for 5 min. The pellet was wash with lysis buffer three times and then eluted with elution buffer (50 mM Tris-HCl (pH 7.5), 150 mM NaCl, 10% glycerol, 250 mM imidazole). The elution fraction was snap frozen with liquid N2 and stored at –80°C.

Liposome preparation

Dehydrated lipids (Avanti Polar Lipids) were dissolved in chloroform and combined in molar ratios described in Table S3. Lipids were dried under vacuum for 2 hr and then rehydrated in HK buffer (25 mM HEPES, pH 7.4, 125 mM KOAc) at 37°C for overnight. Lipids were extruded through 400 nm filters (Whatman) using a miniextruder (Avanti Polar Lipids). Lipids were extruded using 19 passes through the filter and stored at 4°C. Liposomes were used within 1 week of extrusion.

Liposome sedimentation assay

A 40-µL reaction in a 9.5 × 38 mm Polyallomer centrifuge tube (Beckman Coulter cat #357448) containing 250 µM liposomes and ~1 µg purified GFP tagged protein in HK buffer (with 2 mM CaCl2) were incubated at RT for 10 min. Mixtures was spun at 4°C at 55000 rpm for 30 min. Supernatant was removed via pipette immediately and 8 µL of 6x SDS sample buffer was added. Pellets were washed with HK buffer and resuspended with 48 µL of 1x SDS sample buffer (made by diluting 6x SDS sample buffer in HK buffer). All samples were heated at 55°C for 5 min and visualized by SDS-Page/Western Blot.

Western blot

The proteins were separated by 4-20% SDS-PAGE gel (Bio-Rad) and transferred onto nitrocellulose membranes (LiCOR). After blocking with 5% non-fat milk in TBST (Tris-buffered saline with 0.1% Tween 20) at RT for 1 hr, membranes were washed 3 times with TBST for 15 min and incubated with primary antibodies (anti-GFP Rabbit IgG Antibody Fraction, Alexa Fluor® 488 Conjugate, Life Technologies) overnight. ChemiDoc was used for detecting Alexa Fluor® 488.

Image analysis and quantification

Image processing and analyses were done in Fiji/ImageJ or ilastik. For injured dendrites and pruned dendrites marked by *ppk-MApHS*, the pHluorin-positive pixel area in a region of interest (ROI) (ApH), tdTom positive pixel area in the ROI (Atom) were measured and the unengulfment ratio was calculated based on following formula: 100·ApH/Atom. Methods for tracing and measuring C4da neuron dendrite length have been previously described (7). Briefly, the images were segmented by Auto Local Threshold and reduced to single pixel skeletons before measurement of skeleton length by pixel distance. The dendrite debris measurement has been described previously (3). Briefly, a region of interest (ROI) was

generated by including a quadrant of a neuron's territory. Dendrite debris within the ROI was converted to binary masks based on fixed thresholds. Different thresholds were used for *ppk-C4-tdTom* and *ppk-Gal4 UAS-CD-tdTom* as they have different brightness. The debris pixel area (Adeb), and ROI area (AROI) were measured, and dendrite coverage ratio was calculated based on following formula: 100·ADeb/AROI. For measuring debris dispersion of injured dendrites, dendrite debris was segmented by Auto Threshold (the "Default" method) in a rectangular ROI that was previously covered by injured dendrites. The ROI was divided into 15x15-pixel squares. The debris spread index was the area ratio of all squares containing dendrite debris in the ROI. For measuring Orion-GFP and AV-mCard on dendrites, tdTom signals on dendrites were used to generate dendrite masks for measurement of GFP or mCard mean intensities within the masks. For measuring Drpr-GFP recruitment, tdTom signals on dendrites were used to generate dendrite masks to measure total dendrite area (Atot) and GFP-positive area (AGFP). The Drpr recruitment index was calculated based on the formula: AGFP/Atot. For V5 staining, Drpr staining and Orion-GFP binding on epidermal cells, signals on cell boundaries of epidermal cells were measured. For Orion-GFP variant intensities in hemolymph, the signal in a single optical section was measured. For Orion-GFP variant intensities in fat body, maximum projected image was measured.

Statistical Analysis

R was used to conduct statistical analyses and generate graphs. (*$p < 0.05$, **$p < 0.01$, and ***$p < 0.001$). Statistical significance was set at $p < 0.05$. Data acquisition and quantification were performed non-blinded. Acquisition was performed in ImageJ. Statistical analyses were performed using R. We used the following R packages: car, stats, multcomp for statistical analysis and ggplot2 for generating graphs. For the statistical analysis we ran the following tests, ANOVA (followed by Tukey's HSD) when dependent variable was normally distributed and there was approximately equal variance across groups. When dependent variable was not normally distributed and variance was not equal across groups, we used Kruskal-Wallis (followed by Dunn's test, p-values adjusted with Benjamini-Hochberg method) to test the null hypothesis that assumes that the samples (groups) are from identical populations. We used Welch's t-test for comparison between two groups. To check whether the data fit a normal distribution, we generated qqPlots to analyze whether the residuals of the linear regression model are normally distributed. We used the Levene's test to check for equal variance within groups. The quantification of percentages of injured dendrites showing different timings of AV binding was compared using Fisher's exact test.

Replication

For all larval and adult imaging experiments, at least 3 biological replications were performed for each genotype and/or condition.

SI Figures

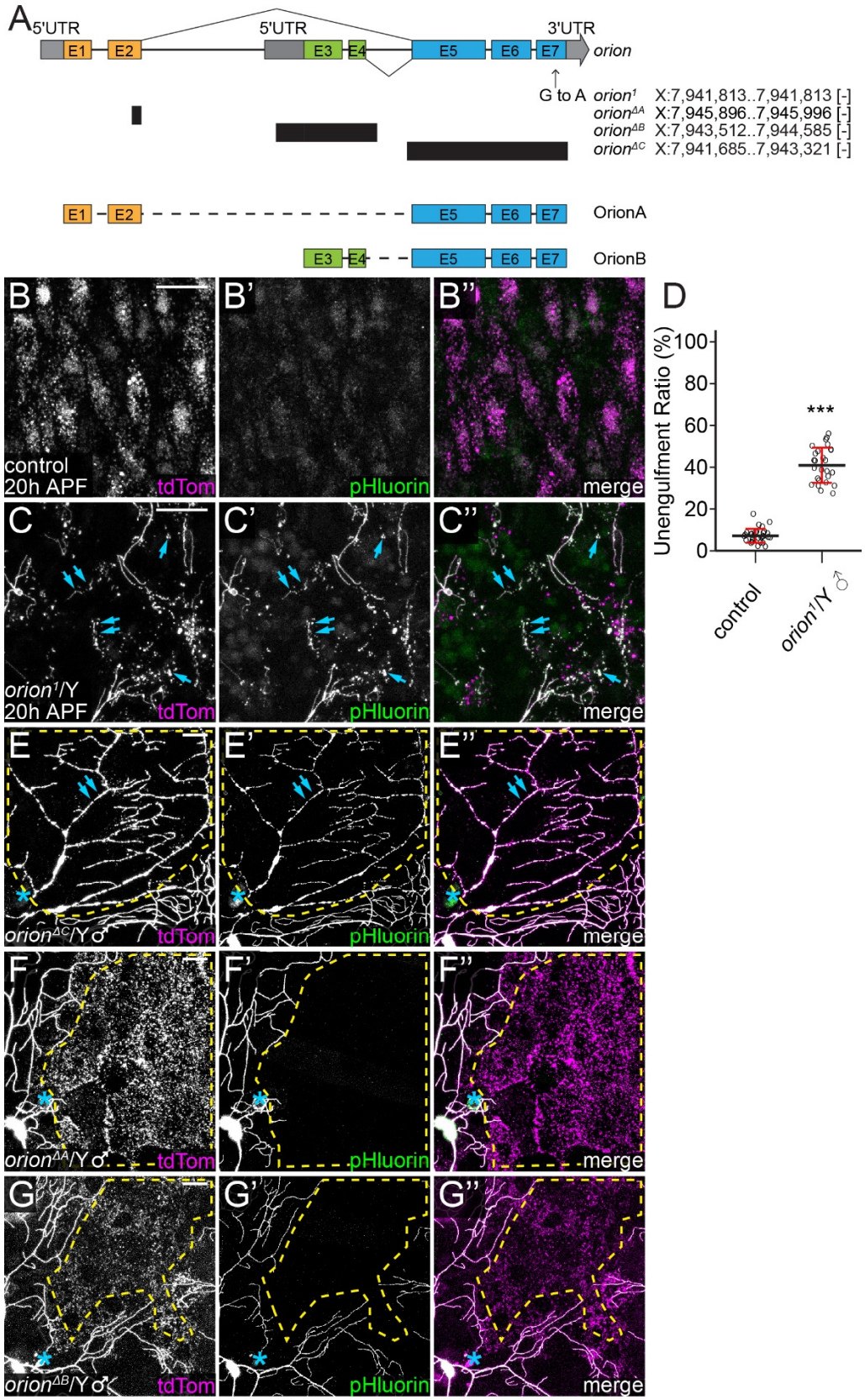
A
5'UTR
5'UTR
3'UTR
E1
E2
E3
E4
E5
E6
E7
orion
G to A
orion¹ X:7,941,813..7,941,813 [-]
orionΔA X:7,945,896..7,945,996 [-]
orionΔB X:7,943,512..7,944,585 [-]
orionΔC X:7,941,685..7,943,321 [-]
OrionA
OrionB
B
B'
B''
control
20h APF
tdTom
pHluorin
merge
C
C'
C''
orion¹/Y
20h APF
D
Unengulfment Ratio (%)
100
80
60
40
20
0
***
control
orion¹/Y ♂
E
E'
E''
orionΔC/Y ♂
F
F'
F''
orionΔA/Y ♂
G
G'
G''
orionΔB/Y ♂

Figure S1: *orion* mutant alleles and engulfment phenotypes

(A) Schematic representation of the *orion* locus in the wildtype and in four different *orion* alleles (*orion*^{1}, *orion*$^{\Delta A}$, *orion*$^{\Delta B}$ and *orion*$^{\Delta C}$). Black bars indicate deleted regions. The two mRNA splicing isoforms of *orion* are also indicated. The *orion* gene annotation is based on Release 6 reference genome assembly.

(B-C") Partial dendritic fields of ddaC neurons at 20 hrs after puparium formation (APF) in wildtype (B-B") and *orion*^{1} hemizygous (C-C") pupae. Blue arrows: unengulfed dendrite fragments.

(D) Quantification of unengulfment ratio of pruned dendrites (area of pHluorin-positive debris/area of tdTom-positive debris) at 19-21 hrs APF. n = number of neurons and N = number of animals: control (n = 30, N = 12); *orion*^{1} hemizygotes (n = 26, N = 9). Welch's t-test; ***p≤0.001; black bar, mean; red bars, SD.

(E-E") Partial dendritic field of a ddaC neuron in *orion*$^{\Delta C}$ hemizygotes at 23 hrs AI. Blue arrows: injured but unengulfed dendrite fragments.

(F-G") Partial dendritic fields of ddaC neurons in *orion*$^{\Delta A}$ hemizygotes (G-G"), and *orion*$^{\Delta B}$ hemizygotes (G-G") at 23-24 hrs AI.

In all image panels, neurons were labeled by *ppk-MApHS*. Scale bars, 25 μm. In (E-G"), yellow dash outlines: territories originally covered by injured dendrites; blue asterisks: injury sites.

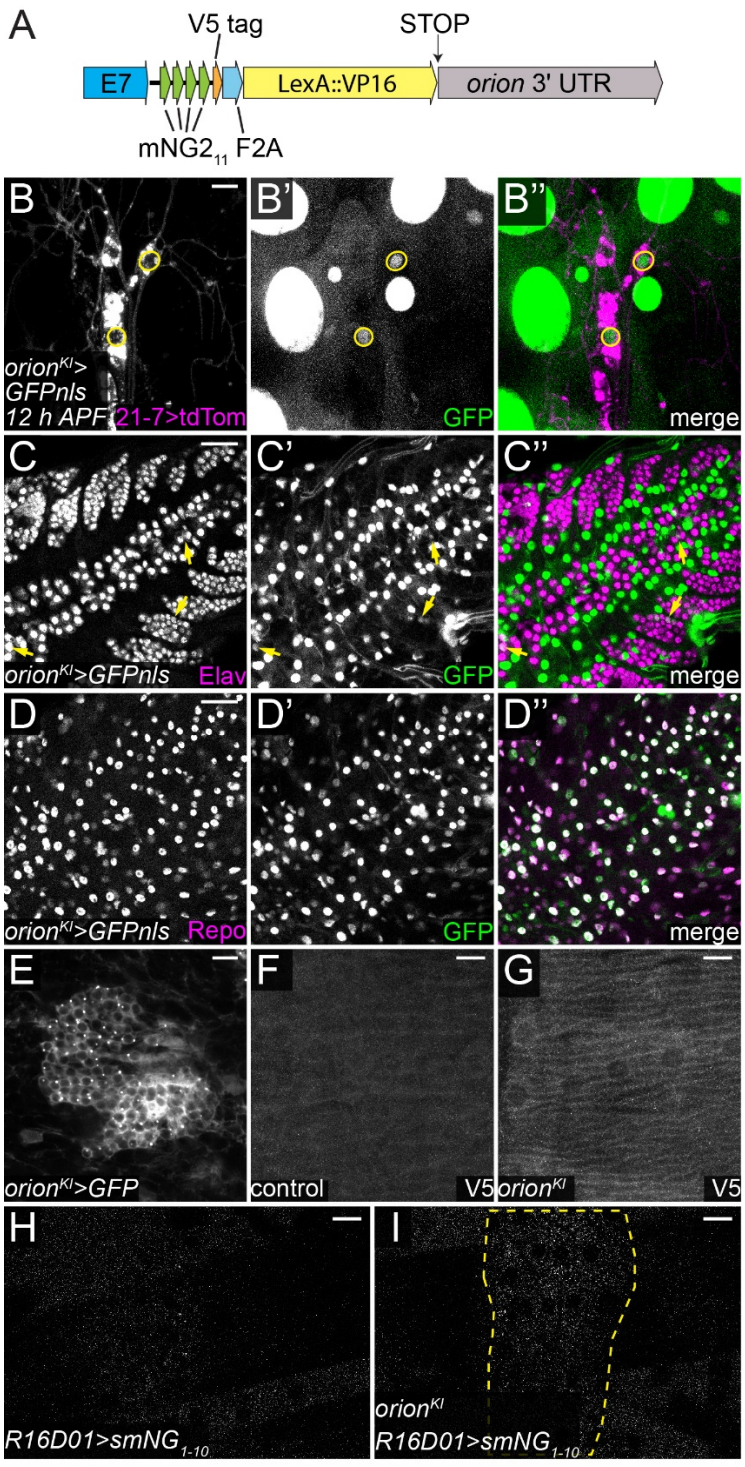

Figure S2: Orion functions cell-non-autonomously

(A) Schematic representation of the *orion^{KI}* allele.

(B-B") GFPnls expression driven by *orion-LexA* in ddaC and ddaE neurons at 12 hrs APF. Yellow circles indicate nuclei of ddaC and ddaE neurons. Neurons were labeled by *21-7-Gal4>CD4-tdTom*.

(C-D”) GFPnls expression driven by *orion-LexA* in the larval ventral nerve cord (VNC). Nuclei of neurons are labeled by Elav staining (C-C”); glial nuclei are labeled by Repo staining (D-D”). Yellow arrows (C-C”): a small number of neurons expressing *orion*.

(E) GFP expression driven by *orion-LexA* in the mushroom body Kenyon cells at 8 hrs APF.

(F-G) V5 staining of larval body walls in the wildtype control (w^{1118}) (F) and $orion^{KI}$ (G).

(H-I) Signals of reconstituted mNG in control (H) and $orion^{KI}$ (I) epidermal cells. Secreted mNG_{1-10} ($smNG_{1-10}$) was expressed in patches of epidermal cells (outlined in H) driven by *R16D01-Gal4*.

Scale bars, 10 μm (B and E) and 25 μm (C-D” and F-I).

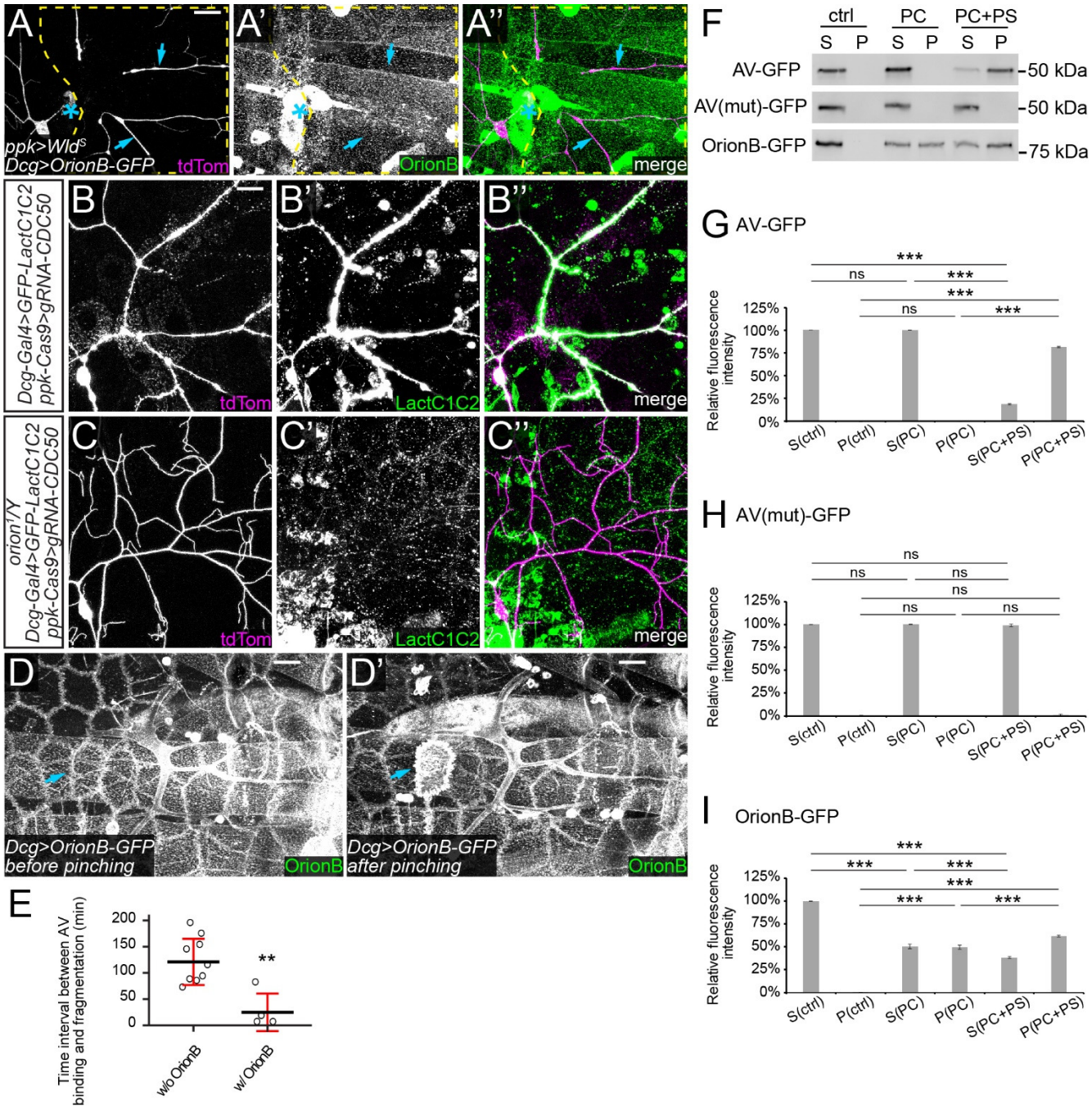

Figure S3: PS exposure induces Orion binding to the cell surface

(A-A") Lack of OrionB-GFP labeling on injured dendrites of a ddaC neuron with Wld^S OE at 6 hrs AI. Yellow dash outlines: territories originally covered by injured dendrites; blue asterisks: injury sites; blue arrows: injured dendrites lacking OrionB-GFP labeling.

(B-C") *CDC50* KO neurons in the presence of fat body-derived GFP-LactC1C2 in control (B-B") and *orion*^{1} hemizygous (C-C") larvae.

(D-D') OrionB-GFP binding on epidermal cells before (D) and after (D') gentle pinching. Blue arrows indicate enhanced OrionB binding.

(E) Time interval between AV binding and dendrite fragmentation for the dendrites showing AV binding. n = number of measurements and N = number of animals: w/o OrionB OE (n = 9, N = 5); w/ OrionB OE (n = 4, N = 2). Welch's t-test.

(F) Western blot of liposome sedimentation assay. Ctrl, control without liposomes; PC, PC-only liposomes; PC+PS, liposomes containing 20% PS; S, supernatant; P, pellet.

(G-I) Quantification of signal intensity of AV-GFP (F), AVmut-GFP (G), and OrionB-GFP (H) in the western blot of liposome sedimentation assay. n=3.

Neurons were labeled by *ppk-CD4-tdTom* (A-C"). In all image panels, scale bars, 25 μm. For all quantifications, **p≤0.01, ***p≤0.001; n.s., not significant. Black bar, mean; red bar, SD.

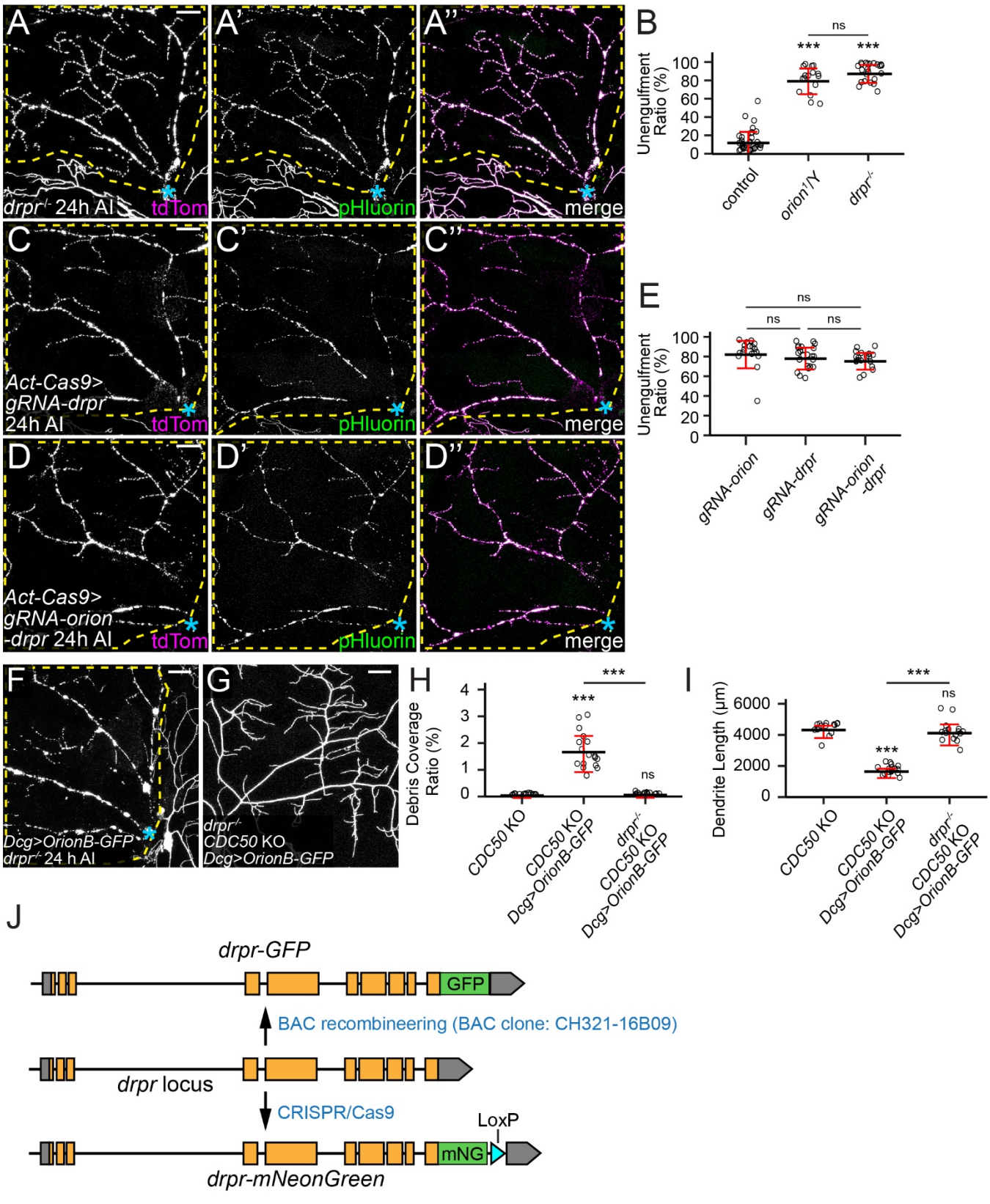

Figure S4: Orion recruits epidermal Drpr to injured dendrites

(A-A") Partial dendritic fields of a ddaC neuron in *drpr*$^{-/-}$ at 24 hrs AI.

(B) Quantification of unengulfment ratio of injured dendrites. n = number of neurons and N = number of animals: control and *orion*^{1}/Y (same dataset as in Figure 1D); *drpr*$^{-/-}$ (n = 23, N = 10). One-way ANOVA and Tukey's test.

(C-D") Partial dendritic fields of ddaC neurons at 24 hrs AI with whole-body *drpr* KO (C-C"), and *drpr*+*orion* double KO (D-D").

(E) Quantification of unengulfment ratio of injured dendrites. n = number of neurons and N = number of animals: *orion* KO (same dataset as in Figure 2L); *drpr* KO (n = 23, N = 12); *orion*+*drpr* double KO (n = 19, N = 10). One-way ANOVA and Tukey's test.

(F) Partial dendritic fields of an injured ddaC neuron with OrionB-GFP OE in fat body in the *drpr*$^{-/-}$ background at 24 hrs AI.

(G) Partial dendritic fields of a *CDC50* KO neuron with OrionB-GFP OE in fat body in the *drpr*$^{-/-}$ background.

(H-I) Quantification of debris coverage ratio (H) and dendrite length (I). n = number of neurons and N = number of animals: *CDC50* KO and *CDC50* KO + *Dcg>OrionB-GFP* (96 hrs AEL, same dataset as in Figure 3K); *drpr*$^{-/-}$ + *CDC50* KO + *Dcg>OrionB-GFP* (120 hrs AEL, n = 16, N = 8). For (H), Kruskal-Wallis (One-way ANOVA on ranks) and Dunn's test, p-values adjusted with the Benjamini-Hochberg method; for (I), one-way ANOVA and Tukey's test; ***p≤0.001; n.s., not significant. The significance level above each genotype is for comparison with the control. Black bar, mean; red bars, SD.

(J) Schematic representation of Drpr-GFP and Drpr-mNG. Yellow boxes indicate exons, grey boxes indicate untranslated regions.

Neurons were labeled by *ppk-MApHS* (A-A", C-D"), and *ppk-CD4-tdTom* (F-G). Scale bars, 25 μm.

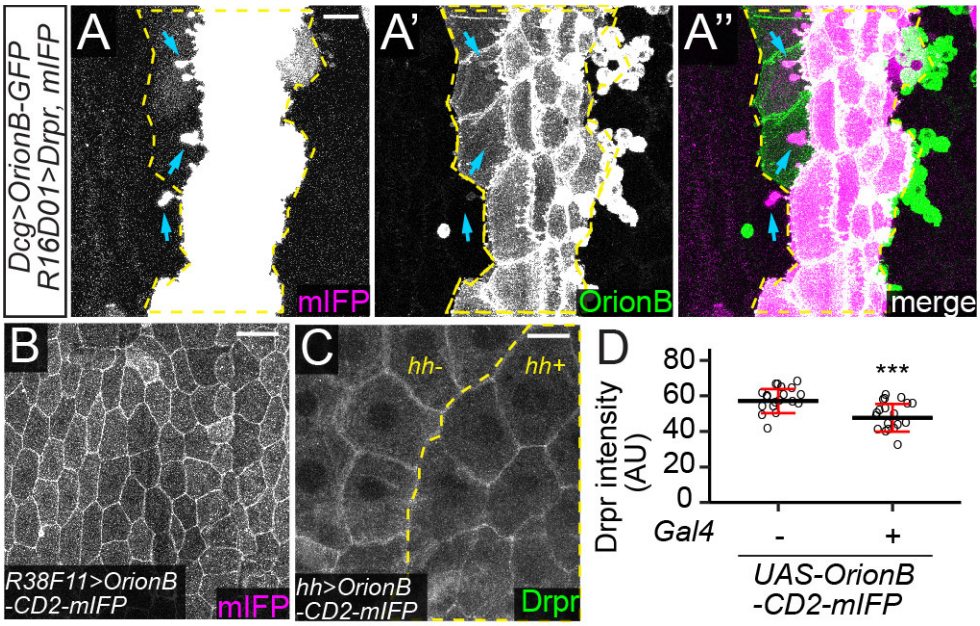

Figure S5: Orion mediates the interaction between PS and Drpr

(A-A") Protrusions (blue arrows) extended from Drpr OE epidermal cells (labeled by mIFP) in the presence of fat body-derived OrionB-GFP. Yellow dash outlines: Drpr OE region.

(B) OrionB-CD2-mIFP localization in epidermal cells driven by *R38F11-Gal4*.

(C) Drpr localization in epidermal cells with OrionB-CD2-mIFP expressed in the *hh* domain. Yellow dash outlines: *hh-Gal4>OrionB-CD2-mIFP* region.

(D) Quantification of stained Drpr levels in epidermal cells with or without OrionB-CD2-mIFP OE. n = number of measurements: w/o OrionB-CD2-mIFP OE (n = 19); w/ OrionB-CD2-mIFP OE (n = 19). Welch's t-test; ***p≤0.001; black bar, mean; red bars, SD.

Scale bars, 25 μm (A-A" and C), 50 μm (B).

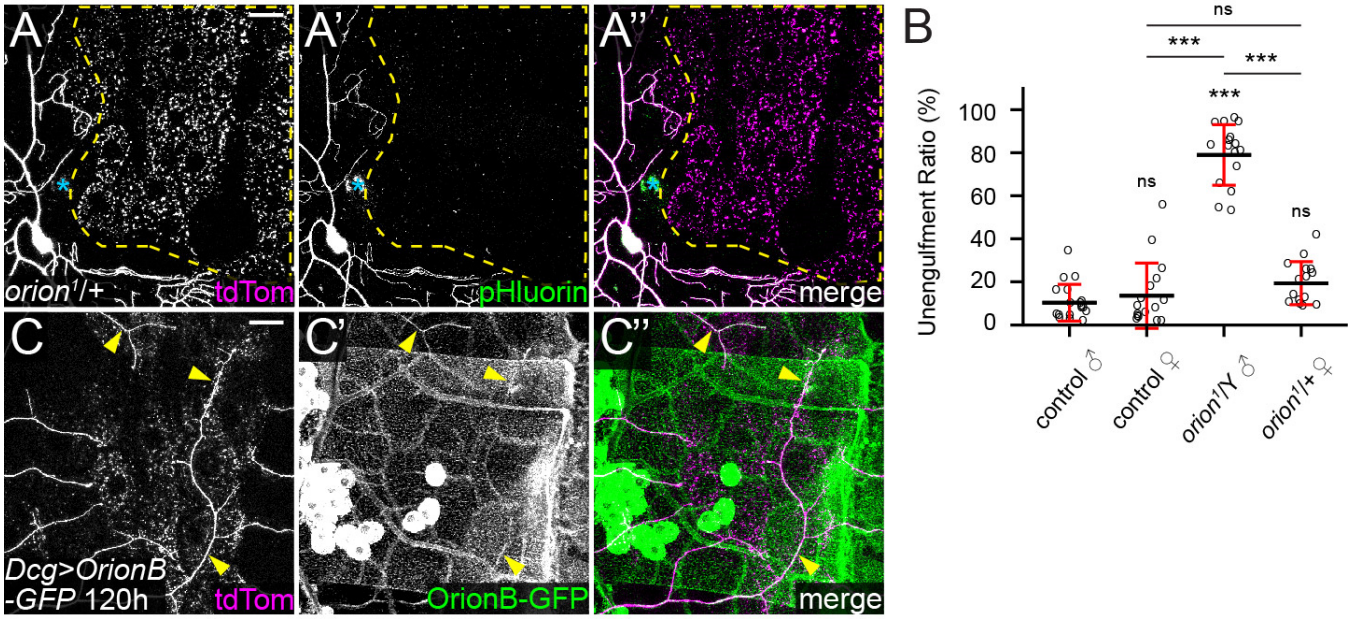

Figure S6: The Orion dosage determines the sensitivity of epidermal cells to PS-exposing dendrites

(A-A") Partial dendritic fields of a ddaC neuron in an *orion*^{1} heterozygous larva at 22 hrs AI. Yellow dash outlines: territories originally covered by injured dendrites; blue asterisks: injury sites.

(B) Quantification of unengulfment ratio of injured dendrites. n = number of neurons and N = number of animals: control males, control females, and *orion*^{1}/Y (same dataset as in Figure 1D); *orion*^{1}/+ (n = 15, N = 8). One-way ANOVA and Tukey's test; ***p≤0.001; n.s., not significant. The significance level above each genotype is for comparison with the control. Black bar, mean; red bars, SD.

(C-C") Partial dendritic fields of a wildtype neuron with OrionB-GFP OE in the fat body at 120 hrs AEL. Yellow arrowheads: OrionB-GFP colocalizing with dendrites.

Neurons were labeled by *ppk-MApHS* (A-A"), and *ppk-CD4-tdTom* (C-C"). For all image panels, scale bars, 25 μm.

SI Tables

Table S1. Key Resource Table

REAGENT or RESOURCE	SOURCE	IDENTIFIER	ADDITIONAL INFORMATION
Experimental Models: Organisms/Strains			
orion^{1}	(6)		
orion$^{\Delta C}$	(6)		
orion$^{\Delta A}$	(6)		
orion$^{\Delta B}$	(6)		
orion-mNG2$_{11x4}$*-V5-T2A-LexA (orion*^{KI}*)*	this study		*orion-mNG(11x4)-F2A-LexA::VP16*$^{7A-1}$
Act5C-Cas9	Bloomington Drosophila Stock Center	RRID:BDSC_54590	*Act5C-Cas9.P*
ppk-MApHS	(16)		*ppk-MApHS*^{1}
UAS-TMEM16F	(3)		*UAS-TMEM16F(D430G)*^{VK00016}
ppk-Gal4	(17)		*ppk-Gal4*^{VK00037}
21-7-Gal4	(18)		*GawB*$^{21-7}$
Dcg-Gal4	(19)		
UAS-AnnexinV-mCard	(3)		*UAS-AnnexinV-mCard*^{VK00037}
UAS-CD4-tdTom	(4)		*UAS-CD4-tdTom*^{7M1}
UAS-OrionB-GFP	this study		*UAS-orion(B)-sfGFP*^{VK00018}
UAS-OrionB-Myc	(6)		*UAS-orion-B-myc*
UAS-CDC50-T2A-ATP8A(E)	this study		*UAS-CDC50-T2A-ATP8A(E)*^{VK00016}
LexAop-OrionB-GFP	this study		*LexAop-orion(B)-sfGFP*^{VK37}
ppk-Cas9	(14)		*ppk-Cas9*^{7D}
UAS-Drpr	Bloomington Drosophila Stock Center	RRID:BDSC_67035	*UAS-drpr[I]*
drpr-GFP	this study		*drpr-sfGFP*^{VK00037}
Dcg-LexA	(20)		
UAS-Drpr^{Cyto}	this study		*UAS-drprTM-smGFP.HA*^{VK00018}
UAS-OrionB-CD2-mIFP	this study		*UAS-Orion(B)-CD2-mIFP*^{VK00019}
UAS-ATP8A	(15)		*UAS-ATP8Acore*^{VK00016}

UAS-OrionB^{AX3C}-GFP	this study		*UAS-orion(B.CX3Cmut)-sfGFP^{VK00018}*
UAS-OrionB^{AAY}-GFP	this study		*UAS-orion(B.RRYmut)-sfGFP^{VK00018}*
UAS-OrionB^{1}-GFP	this study		*UAS-orion(B.G611D)-sfGFP^{VK00018}*
UAS-AVmut-GFP	(3)		*UAS-AnnexinV(mut)-GFP^{VK00018}*
ppk-Cas9	(14)		*ppk-Cas9^{7D}*
gRNA-CDC50	(3)		*gRNA-CDC50^{attP2}*
gRNA-Nmnat	(15)		*gRNA-NmnatVK00027*
LexAop-GFPnls	Bloomington Drosophila Stock Center	RRID:BDSC_29955	*lexAop-2xhrGFP.nls^{3a}*
gRNA-orion	this study		*gRNA-orion(BR)^{VK00027}*
shot-Cas9	(15)		*shot-Cas9^{1A}*
SOP-Cas9	(14)		*[sc-E1]x8-Cas9^{3A}*
R16D01-Gal4	Bloomington Drosophila Stock Center	RRID: BDSC_48722	*R16D01-Gal4^{attP2}*
UAS-smNG$_{1-10}$	this study		*UAS-smNG2(1-10)^{VK00027}*
ppk-LexA	(7)		*ppk-LexA.GAD^{3}*
LexAop-Wld^{S}	(15)		*LexAop-WldS^{VK00027}*
ppk-CD4-tdTom	(4)		*ppk-spGFP11-CD4-tdTom^{2}*
R16A03-LexA	(3)		*R16A03-LexAp65^{VK00027}*
UAS-mIFP-T2A-HO1	(7)	RRID: BDSC_64181	*UAS-mIFP-T2A-HO1^{VK00005}*
UAS-GFP-LactC1C2	(3)		*UAS-GFP-LactC1C2^{VK00018}*
drpr^{-}	(3)		*drpr^{indel3}*
gRNA-drpr	(15)		*gRNA-drpr(BR)^{VK00027}*
gRNA-orion-drpr	this study		*gRNA-orion-drpr(BR)^{VK00027}*
hh-Cas9	(14)		*R28E04-Cas9^{6A}*
drpr-mNG	this study		*drpr-mNeonGreen$^{1008-15}$*
UAS-Drpr	(8)		*UAS-drpr[I]:HA*
R38F11-Gal4	Bloomington Drosophila Stock Center	RRID: BDSC_50014	*R38F11-Gal4^{attP2}*
gRNA-ATP8A	(3)		*gRNA-ATP8A^{VK00019}*
hh-Gal4	(21)		
Dp(1:3)DC496	Bloomington Drosophila Stock Center	RRID:BDSC_33489	*PBac{DC496}^{VK00033}*

ppk-Gal4	(17)		*ppk-Gal4^{1a}*
UAS-CD4-tdTom	(4)		*UAS-CD4-tdTom^{VK00033}*
y^{1} w^{67c23} Cre(y+)^{1b}; D/TM3, Sb^{1}	Bloomington Drosophila Stock Center	RRID:BDSC_851	
y^{1} nos-Cas9^{ZH-2A} w*	Bloomington Drosophila Stock Center	RRID:BDSC_54591	
13XLexAop2-6XGFP	Bloomington Drosophila Stock Center	RRID:BDSC_52266	*13XLexAop2-6XGFP^{attP2}*
Act-Cas9 w lig4	Bloomington Drosophila Stock Center	RRID:BDSC_58492	*y^{1} Act5C-Cas9(RFP-)$^{ZH-2A}$ w^{1118} DNAlig4^{169}*
Recombinant DNA			
pAC-CR7T-gRNA2.1-nlsBFP	(1)	RRID:Addgene_170515	
pUC57-50-GS-FRTGFP2ALexAVP16-50	(2)		
LD24308	*Drosophila* Genomics Resource Center		
pIHEU-MCS	(3)	RRID:Addgene_58375	
pACU	(4)	RRID:Addgene_58373	
pENTR-orionB-AX3C	(6)		
pAPLO	(7)	RRID:Addgene_112805	
pCAG-smFP-HA	(9)	RRID:Addgene_59759	
GH28327	*Drosophila* Genomics Resource Center		
NB40 cDNA library	(10)		
CH321-16B09	BACPAC Resources Center		
pGalK	(11)		
pHD-DsRed	Addgene	RRID:Addgene_51434	
pCFD4-U6.1_U6.3	(13)	RRID:Addgene_49411	
pAC-U63-QtgRNA2.1-BR	(1)	RRID:Addgene_170513	
Bacterial Strains			
SW102	(11)		
EPI300	Lucigen Corporation	Cat. # C300C105	
Antibody			

Rat-Elav-7E8A10 (1:20)	Developmental Studies Hybridoma Bank	AB_528218	
8D12 anti-Repo (1:20)	Developmental Studies Hybridoma Bank	AB_528448	
V5 Tag Antibody (R960-25) (1:400)	Thermo Fisher Scientific	AB_2556564	
Rabbit anti Drpr polyclonal (1:100)	(22)		
Cy™5 AffiniPure Donkey Anti-Rat IgG (H+L) (1:200)	Jackson ImmunoResearch Labs	AB_2340671	712-175-150
Alexa Fluor® 647 AffiniPure Donkey Anti-Mouse IgG (H+L) (1:200)	Jackson ImmunoResearch Labs	RRID: AB_2340862	715-605-150
Alexa Fluor® 488 AffiniPure Donkey Anti-Rabbit IgG (H+L) (1:200)	Jackson ImmunoResearch Labs	RRID: AB_2313584	711-545-152
Alexa Fluor® 488 AffiniPure Donkey Anti-Mouse IgG (H+L) (1:400)	Jackson ImmunoResearch Labs	RRID: AB_2340846	715-545-150
anti-GFP Rabbit IgG Antibody Fraction, Alexa Fluor® 488 Conjugate	Life Technologies	Catalog # A-11122	
Software and Algorithms			
Fiji	https://fiji.sc/	RRID: SCR_002285	
R	https://www.r-project.org/	RRID: SCR_001905	
Adobe Photoshop	Adobe	RRID:SCR_014199	
Adobe Illustrator	Adobe	RRID:SCR_010279	
ilastik	(23)		
UCSF Chimera	(24)		
Other			
NEBuilder® HiFi DNA Assembly Master Mix	New England Biolabs Inc.	#E2621	
HisPur™ Ni-NTA Resin	ThermoFisher Scientific	88221	
6xHis nanobody	Addgene	#49172	
Protease Inhibitor Cocktail 50X	Promega	G6521	
AEBSF Protease Inhibitor	ThermoFisher Scientific	78431	
2.8 mm Ceramic beads bulk, 325 g	Omni International	19-646	
Bead ruptor 4	Omni International	25-010	
TritonX-100	Amresco	M143	Proteomics Grade

1,2-dioleoyl-sn-glycero-3-phosphocholine (DOPC)	Avanti Polar Lipids, Inc.	Cat# 850375	
1,2-dioleoyl-sn-glycero-3-phospho-L-serine (DOPS) sodium salt	Avanti Polar Lipids, Inc.	Cat# 840035	
1,1'-Dioctadecyl-3,3,3',3'-Tetramethylindotricarbocyanine Iodide (DiR'; DilC18(7))	ThermoFisher Scientific	Cat# D12731	
Whatman® Nuclepore™ Track-Etched Membranes	Millipore Sigma	WHA110657	
Extruder Set With Holder/Heating Block	Avanti Polar Lipids, Inc.	610000-1EA	
9.5 × 38 mm Polyallomer centrifuge tube	Beckman Coulter	Cat #357448	
4–20% Mini-PROTEAN® TGX™ Precast Protein Gels, 12-well, 20 µl	Bio-Rad	#4561095	
Odyssey® Nitrocellulose Membranes	LI-COR	P/N 926-31092	
ChemiDoc Imaging System	Bio-Rad	17001401	

Table S2. gRNA target sequences.

Gene	Target sequence 1	Target sequence 2
orion (for KO)	GAAGGGCAACTACACCCAGG	CATGTTTCGTCGGATCACAG
orion (for KI)	GATTCTAAAGCGGAGAGAAG	
drpr (for KO)	CCATGCCGTAGAATCCAGGT	ACGGACAAGGATGCGCCCAG
drpr (for KI)	AGAAATTTCGGACTGGAACT	GCCGGAACAGTCACTTCACC

Table S3 Composition of liposomes

Lipid	Composition
PC	DOPC 99%, DiR dye 1%;
PC+PS	DOPC 79%, DOPS 20%, DiR dye 1%

SI Movie Legends

Movie S1 (separate file). OrionB-GFP labels degenerating dendrites after injury, related to Figure 3.

Time-lapse movie of laser-injured ddaC dendrites from 2.5 to 11 hrs AI, showing OrionB-GFP labeling on injured dendrites. The dendrite arbor on the bottom right was injured while the ones at the top were not. The mobile cells in the OrionB-GFP channel are hemocytes. Time stamp is relative to the first frame.

Movie S2 (separate file). AV-mCard labels injured dendrites before dendrite fragmentation, related to Figure 3.

Time-lapse movie of laser-injured ddaC dendrites from 2.5 to 5 hrs AI, showing AV-mCard labeling on injured dendrites as early as 2 hrs before fragmentation. The AV-mCard signals that do not colocalize with tdTom signals indicate AV-mCard labeling on injured dendrites of other types of neurons. Time stamp is relative to the frame of dendrite fragmentation.

Movie S3 (separate file). AV-mCard fails to label injured dendrites when OrionB-GFP is co-expressed, related to Figure 3.

Time-lapse movie of laser-injured ddaC dendrites from 1 to 3 hrs AI showing OrionB-GFP labeling but not AV-mCard labeling on injured dendrites before fragmentation. Time stamp is relative to the frame of dendrite fragmentation.

SI References

1. Koreman GT*, et al.* (2021) Upgraded CRISPR/Cas9 tools for tissue-specific mutagenesis in Drosophila. *Proc Natl Acad Sci U S A* 118(14).
2. Chen Y*, et al.* (2014) Cell-type-specific labeling of synapses in vivo through synaptic tagging with recombination. *Neuron* 81(2):280-293.
3. Sapar ML*, et al.* (2018) Phosphatidylserine Externalization Results from and Causes Neurite Degeneration in Drosophila. *Cell Rep* 24(9):2273-2286.
4. Han C, Jan LY, & Jan YN (2011) Enhancer-driven membrane markers for analysis of nonautonomous mechanisms reveal neuron-glia interactions in Drosophila. *Proc Natl Acad Sci U S A* 108(23):9673-9678.
5. Yu D*, et al.* (2015) A naturally monomeric infrared fluorescent protein for protein labeling in vivo. *Nat Methods* 12(8):763-765.
6. Boulanger A*, et al.* (2021) Axonal chemokine-like Orion induces astrocyte infiltration and engulfment during mushroom body neuronal remodeling. *Nat Commun* 12(1):1849.
7. Poe AR*, et al.* (2017) Dendritic space-filling requires a neuronal type-specific extracellular permissive signal in Drosophila. *Proc Natl Acad Sci U S A* 114(38):E8062-E8071.
8. Logan MA*, et al.* (2012) Negative regulation of glial engulfment activity by Draper terminates glial responses to axon injury. *Nat Neurosci* 15(5):722-730.
9. Viswanathan S*, et al.* (2015) High-performance probes for light and electron microscopy. *Nat Methods* 12(6):568-576.

10. Brown NH & Kafatos FC (1988) Functional cDNA libraries from Drosophila embryos. *J Mol Biol* 203(2):425-437.

11. Warming S, Costantino N, Court DL, Jenkins NA, & Copeland NG (2005) Simple and highly efficient BAC recombineering using galK selection. *Nucleic Acids Res* 33(4):e36.

12. Shaner NC*, et al.* (2013) A bright monomeric green fluorescent protein derived from Branchiostoma lanceolatum. *Nat Methods* 10(5):407-409.

13. Port F, Chen HM, Lee T, & Bullock SL (2014) Optimized CRISPR/Cas tools for efficient germline and somatic genome engineering in Drosophila. *Proc Natl Acad Sci U S A* 111(29):E2967-2976.

14. Poe AR*, et al.* (2019) Robust CRISPR/Cas9-Mediated Tissue-Specific Mutagenesis Reveals Gene Redundancy and Perdurance in Drosophila. *Genetics* 211(2):459-472.

15. Ji H, Sapar ML, Sarkar A, Wang B, & Han C (2022) Phagocytosis and self-destruction break down dendrites of Drosophila sensory neurons at distinct steps of Wallerian degeneration. *Proc Natl Acad Sci U S A* 119(4).

16. Han C*, et al.* (2014) Epidermal cells are the primary phagocytes in the fragmentation and clearance of degenerating dendrites in Drosophila. *Neuron* 81(3):544-560.

17. Han C*, et al.* (2012) Integrins regulate repulsion-mediated dendritic patterning of drosophila sensory neurons by restricting dendrites in a 2D space. *Neuron* 73(1):64-78.

18. Song W, Onishi M, Jan LY, & Jan YN (2007) Peripheral multidendritic sensory neurons are necessary for rhythmic locomotion behavior in Drosophila larvae. *Proc Natl Acad Sci U S A* 104(12):5199-5204.

19. Suh JM*, et al.* (2006) Hedgehog signaling plays a conserved role in inhibiting fat formation. *Cell Metab* 3(1):25-34.

20. Karuparti S, Yeung AT, Wang B, Guicardi PF, & Han C (2023) A toolkit for converting Gal4 into LexA and Flippase transgenes in Drosophila. *G3 (Bethesda)*.

21. Han C, Belenkaya TY, Wang B, & Lin X (2004) Drosophila glypicans control the cell-to-cell movement of Hedgehog by a dynamin-independent process. *Development* 131(3):601-611.

22. Freeman MR, Delrow J, Kim J, Johnson E, & Doe CQ (2003) Unwrapping glial biology: Gcm target genes regulating glial development, diversification, and function. *Neuron* 38(4):567-580.

23. Berg S*, et al.* (2019) ilastik: interactive machine learning for (bio)image analysis. *Nat Methods* 16(12):1226-1232.

24. Pettersen EF*, et al.* (2004) UCSF Chimera--a visualization system for exploratory research and analysis. *J Comput Chem* 25(13):1605-1612.